

# Charge Transport in Sb-doped SnO<sub>2</sub> Nanoparticles Studied by THz Spectroscopy

Volodymyr Skoromets<sup>1</sup>, Hynek Němec<sup>1</sup>, Kristina Peters<sup>2</sup>, Dina Fattakhova-Rohlfing<sup>2</sup>, and Petr Kužel<sup>1</sup>

<sup>1</sup>Institute of Physics, Academy of Sciences of the Czech Republic, Prague, 18221 Czech Republic

<sup>2</sup>Department of Chemistry and Biochemistry, University of Munich, Munich, 81377 Germany

**Abstract**—Using terahertz spectroscopy we investigate the charge transport in Sb-doped SnO<sub>2</sub> nanoparticles pressed into pellets. Doped and undoped samples are shown to have different mechanisms of intrinsic conductivity. We systematically study the influence of annealing on intra- and inter-nanoparticle charge transport.

## I. INTRODUCTION

TERAHERTZ (THz) spectroscopy is a pertinent tool for investigations of charge transport in weakly conducting materials as it enables contactless and broadband phase-sensitive probing of the material conductivity. We employ time-domain THz spectroscopy supplemented with appropriate theoretical models to get an insight into the charge transport mechanisms in pellets made of undoped and antimony-doped (up to 10 %) tin-oxide nanoparticles synthesized via solvothermal reaction in tert-butanol [1]. Further technological steps then follow: annealing at 200 or 500 °C, pressing into pellets and optionally a second annealing at 200 or 500 °C. We study in detail how annealing conditions influence the charge transport within individual nanoparticles and between them.

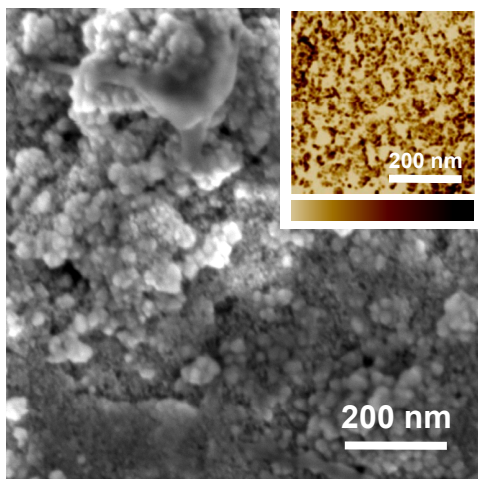


**Fig. 1.** SEM image of one of the 10%-doped samples. Inset: Local current map measured by PeakForce C-AFM. The scale of the current value is below: from 0 (bright edge) to 25 pA (dark edge).

Since the samples are inhomogeneous (see Fig. 1) our analysis of the measured spectra (see examples in Fig. 2) must involve two steps. In the first one, we developed a model for the microscopic conductivity, i.e., a response to the local THz electric field. In the second step, we took into account depolarization fields which define the relation between the incident THz pulse and the local field. The size of the nanoparticles forming pellets is much smaller than the probing wavelength, we could, therefore, employ the effective medium approximation to link the microscopic response to the

macroscopic one.

## II. RESULTS

To model the microscopic response of the nanoparticles we expressed their complex permittivity  $\epsilon(f)$  as a sum of two separate contributions:

$$\epsilon(f) = \epsilon_v(f) + \Delta\epsilon(f),$$

where  $\epsilon_v(f)$  is the contribution of the lattice vibrations and  $\Delta\epsilon(f)$  is the contribution due to the conduction of charges. The essential part of the lattice contribution to the permittivity in the THz range is given by three lowest-frequency phonon modes. Their parameters were taken from the literature [2].

We found that the conduction mechanisms depend on the doping and on the preparation procedure of the nanoparticles and pellets. We distinguished two types of transport mechanisms. (i) The undoped nanoparticles show hopping type conductivity which can be understood as a superposition of relaxations with very broad distribution of relaxation times. To describe such kind of response we used the random free-energy barrier model [3]. (ii) In the case of the doped nanoparticles we revealed that a band-like conduction of free charges is the most appropriate mechanism. We calculated the conductivity using Monte-Carlo method [4], which takes into account microscopic properties of the material including nanoparticle size, mean carrier scattering in the volume of nanoparticles and efficiency of inter-nanoparticle transport.

The measured effective permittivity exceeded 4.5 in all samples. Such a high value cannot be achieved in an ensemble of isolated SnO<sub>2</sub> spheres with air voids [1]. Therefore, we conclude that the investigated nanoparticles (both undoped and doped) form a network with a high degree of dielectric percolation. This fact is also supported by the measurements of local current using conductive AFM (C-AFM, inset of Fig. 1). In the figure one can see many areas with dark color where an electrical current flows through the entire thickness (~0.15 mm) of the pellets. Note that there are some places on the surface with substantially lower conductivity indicating that limited areas of the pellets are electrically isolated from the rest.

In this view we used a modification of the Maxwell-Garnett model to describe our samples, in which a material is composed of a conducting percolated matrix and of non-conducting isolated inclusions. Actually this model describes a conductor containing voids with a well-defined shape. In practice, such a topology does not essentially differ from a percolated network of particles in contact with each other.

For undoped samples the dielectric contribution due to lattice vibrations dominates the contribution of charge transport. Nevertheless, the undoped samples show weak hopping-type conductivity which also perfectly correlates with their very low dc conductivity. We suggest that there are

impurities or imperfections in the undoped material which are responsible for the hopping conduction.

THz conductivity spectra of the doped samples have the real part starting at small non-zero values at low frequencies and increasing towards higher frequencies (Fig. 2). Such spectral behavior is a signature of charge localization either as a result

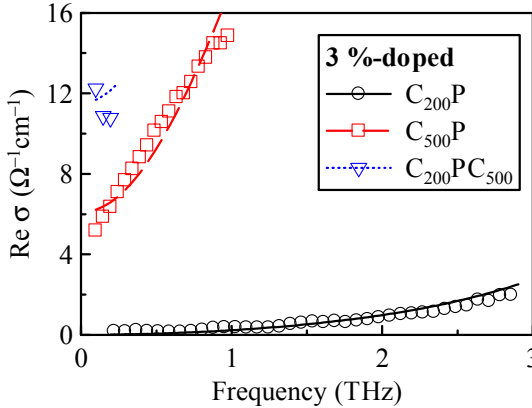


**Fig. 2.** Spectra of the real conductivity of 3 %-doped samples after various technological sequences:  $C_{200}$  and  $C_{500}$  mean calcination at 200°C and 500°C, respectively; P means pelletization. Lines are fits by the developed model.

of the charge confinement or as a manifestation of the depolarization fields.

We found that the doped samples show a band-like conduction of charges inside the nanoparticles. Our fitting function is based on the conductivity calculated using the Monte-Carlo method and it also accounts for the porosity of the pellets and the phonon modes in  $\text{SnO}_2$  (lines in Fig. 2).

Calcination of undoped samples does not noticeably change their THz response. However, calcination of the doped samples leads to dramatic changes in the THz (and dc) response. Calcination at 200°C before pressing ( $C_{200}\text{P}$ ) results in a poor intra-nanoparticle conductivity (circles in Fig. 1) and in a very limited inter-nanoparticles transport. The sub-THz conductivity values are almost two orders of magnitude higher than the measured dc conductivity (cf. Table 1); obviously, there are barriers effectively suppressing charge transport between nanoparticles.

Calcination at 500°C before pressing ( $C_{500}\text{P}$ ) enhances the intrinsic conductivity of the nanoparticles (squares in Fig. 1) and increases also the conductivity of the contact area between the nanoparticles, but the interface resistance still remains rather high, which limits the dc conductivity.

Additional calcination after pressing ( $C_{200}\text{PC}_{500}$ ) leads to a significant increase in the effective THz conductivity. Both the intra-nanoparticle (triangles in Fig. 1) and the dc conductivity are improved. Altogether, this leads to a high THz absorption of the samples above 0.2 THz. However, the dc conductivity is about an order of magnitude lower than the effective THz conductivity (cf. Table 1). This indicates that energy barriers suppressing the long-range charge transport are still present in the material.

Sample	$\frac{\sigma_{\text{dc}}}{\Omega^{-1} \text{cm}^{-1}}$	$\frac{\sigma_{\text{eff}}(0.2 \text{ THz})}{\Omega^{-1} \text{cm}^{-1}}$
$C_{200}\text{P}-3\%$	$(0.8 \div 4) \times 10^{-3}$	0.18
$C_{200}\text{P}-5\%$	$1.6 \times 10^{-3}$	0.12
$C_{200}\text{P}-10\%$	$(0.3 \div 1.1) \times 10^{-3}$	0.14
$C_{500}\text{P}-3\%$	0.33	6
$C_{500}\text{P}-5\%$	0.60	10
$C_{500}\text{P}-10\%$	0.68	7
$C_{200}\text{PC}_{500}-3\%$	0.5	11
$C_{200}\text{PC}_{500}-5\%$	1.5	
$C_{200}\text{PC}_{500}-10\%$	1.0	8
$C_{500}\text{PC}_{500}-3\%$	62	
$C_{500}\text{PC}_{500}-5\%$	40	
$C_{500}\text{PC}_{500}-10\%$	22	

**Table 1.** Conductivities of the doped samples.

Finally, the contact resistance between nanoparticles is almost completely eliminated when the samples are annealed at 500°C both before and after pelletization ( $C_{500}\text{PC}_{500}$ ). The observed dc conductivity of  $62 \Omega^{-1} \text{cm}^{-1}$  makes these samples completely opaque in the THz range.

It is worth mentioning that the dc conductivity does not vary substantially with doping and remains much lower than the THz one. This supports the conclusion that the dc conductivity is controlled mainly by interfaces rather than by the conductivity inside the nanoparticles. Elimination of the barriers is thus one of the important technological issues for the optimization of the dc conductivity of these materials.

### III. SUMMARY

We investigated charge transport in pellets made of undoped and Sb-doped  $\text{SnO}_2$  nanoparticles using time-domain terahertz spectroscopy. We concluded that the nanoparticles form a dielectrically percolated network. Undoped samples show a hopping-type conductivity whereas the Sb-doping introduces band-like conduction inside the nanoparticles. Calcination of doped samples at low temperatures (200°C) leads to a poor intra-nanoparticle conductivity and to a very limited inter-nanoparticle charge transport. Calcination at elevated temperatures (500°C) enhances the conductivity inside the nanoparticles and improves the conductivity of the contact area between nanoparticles. The best conductivity is achieved for samples calcined at 500°C both before and after pressing: the intra-nanoparticle conductivity remains high whereas barriers limiting charge transport between the nanoparticles are largely eliminated.

### REFERENCES

- [1] K. Peters et al., “Water-dispersible electrically conducting antimony-doped tin oxide nanoparticles,” *Chem. Mater.*, 27(3), pp. 1090–1099, 2015.
- [2] P. D. Borges, L. M. R. Scelfaro, H. W. L. Alves, and E. F. da Silva Jr., “DFT study of the electronic, vibrational, and optical properties of  $\text{SnO}_2$ ,” *Theor. Chem. Acc.*, vol. 126, 39, 2010.
- [3] J. C. Dyre, “The random free-energy barrier model for ac conduction in disordered solids,” *J. Appl. Phys.*, vol. 64, 2456, 1988.
- [4] H. Němec et al., “Far-infrared response of free charge carriers localized in semiconductor nanoparticles,” *Phys. Rev. B*, vol. 79, 115309, 2009.